Motion of Small Spherical Particles in an Arbitrary Oriented Cluster Due to the Microwave Propagation

Aslan Nouri Moqadam, Ali Pourziad*, and Saeid Nikmehr

Abstract—The electromagnetic (EM) waves influence substances involved in the propagation medium which leads to deviation or modification. Atomic stresses and strains caused by EM radiation make electromagnetic waves able to stir small particles by exertion of Lorentz force on them which is employed to deviate particles in this paper. The particles are considered as millimeter and micrometer-sized spheres with random electrical properties. Generalized Multi-Particle Mie theory (GMMT) is used to calculate scattering parameters such as Radar Cross Section for aggregates of arbitrarily oriented particles. The direction of motion caused by exerted Lorentz force on particles is accurately obtained in terms of Discrete Dipole Approximation (DDA). A bulk model based on Effective Medium Theory is designed to analyze the scattering parameters of particles, much smaller than incident wavelength. Application of this model is validated by several simulations. The profile of arbitrary incident wave and its amplitude and polarization effects on deviation are investigated, respectively. Numerical results are derived for various arbitrary orientations and different electromagnetic conditions.

1. INTRODUCTION

Scattering of EM waves and their applications are among the most interesting topics in communicational literature. Deviation and modification power of EM waves on much smaller particles tha incident wavelength innovated a new era in the ISM applications. Modification and elimination of cancer tumors in radiotherapy through microwaves besides environmental protection from floating dust particles are the most noticeable applications in medical and industrial societies. Satellite communications and microwave propagation through the atmosphere are also involved with floating atmosphere particles such as rain drops which deviate propagating wave from its main path causing communication loss. Detailed scattering properties of particles in a cluster give incredible information about material, motion and orientation of particles. The reason behind cluster investigation is that small particles are available in different clusters in nature, and accordingly, scattering parameters analysis of an isolated extra small particle is not practical. So, EM waves are widely employed in ISM applications leading to electromagnetic techniques in healthcare and environmental protection.

EM waves facing discontinuities or waves propagating through anisotropic medium deviate from their original paths [1]. This phenomenon, called *scattering*, is an atomic event where positive and negative charges are replaced due to EM wave, so this movement leads to an oscillation. This atomic oscillation tends to radiate, and the primary wave transforms to multiple waves, propagating in different paths [2].

Several techniques were employed to analyze multiple scatterings by arbitrarily shaped particles. Scattering by a single homogenous sphere with the size comparable to wavelength known as the *Mie Theory* is the basic theory for spherical particles [2]. EM scattering by aggregates of spheres with

* Corresponding author: Ali Pourziad (Pourziad@gmail.com).
The authors are with the Antenna and Microwave Laboratory, Department of Electrical and Computer Engineering, The University of Tabriz, Tabriz, Iran.

the help of generalized Multi-particle Mie Theory (GMMT) was studied in late 20s [3]. That is also applicable to variously shaped small particles [4]. Transition Matrix provides expressions for scattering by random shapes such as finite cylinders and spheres, which has been derived for ensemble of spheres by Mishchenko et al. [5]. Ryleigh and discrete dipole approximation (DDA) for EM scattering from small particles compared to wavelength were also employed to study multiple scattering [6].

Environmental application of multiple scatterings were discussed in various papers. Expressions for attenuation and phase shift coefficients for a medium with sand and dust have been demonstrated recently [7]. Radiation pressure of the Sun on fluffy dust particles was calculated by Kimura et al. where the reaction of sun rays propagation through fluffy dust particles and radiation pressure on them were considered [8]. These studies are mostly based on optical frequencies, and the common case is motion of particles in the presence of laser beam [9]. Particles behaviors at microwave frequencies have rarely been discussed in literature and almost ignored.

In this paper, microwave propagation in a random medium and scattering properties of particles which are considered as spheres are investigated by the help of multiple scattering analysis methods. The absolute value and direction of forces exerted on particles are demonstrated in detail. So the motion and movement of particles due to electromagnetic forces exerted on particles can be predicted. The influence of wave polarization and amplitude besides different wave types on the amount and direction of exerted forces will be discussed in later sections. Concerning these effects, proper wave features can be chosen to deviate the spherical particles consciously according to desired application.

2. STATEMENT OF THE PROBLEM

Suppose a system of L isotropic and homogenous spheres confined in a finite volume with specific radius a^l where $l = 1, 2, 3, \ldots, L$ and known electrical permittivity ε^l in which the spheres are arbitrarily oriented. Scattering cross section of the spheres is calculated through a GMMT based algorithm coded by MATLAB software. The purpose of this paper is to deviate these spheres and predict the direction of deviation. The absolute value of forces exerted on spheres besides direction of deviation will be shown in later sections. Some hints about conscious deviation proposed in this paper are suitable for environmental and medical applications.

2.1. Generalized Multi-Particle Mie Theory

Mie Theory is the exact solution for scattering of an isotropic, homogenous sphere lightened by an electromagnetic plane wave. GMMT is not limited to a single sphere, so multi-sphere system can be analyzed in this way. Isolated spheres besides spheres interaction in scattering should be noticed in GMMT [10]. In the Cartesian coordinate system originated in lth sphere center, incident wave on each sphere is the sum of main excitation wave and the wave scattered by other spheres. Vector spherical wave functions (VSWF) are employed to expand scattered, internal and incident electromagnetic fields. Expansion coefficient in each term of GMMT can be calculated based on classical Mie coefficients [1]:

$$E_{inc}^l = -E_0 \sum_{n=1}^{\infty} \sum_{m=-n}^{n} i^{n+1} \left[p_{mn}^l \bar{N}_{mn}^{(1)l} + q_{mn}^l \bar{M}_{mn}^{(1)l} \right],$$

$$E_{sca}^l = E_0 \sum_{n=1}^{\infty} \sum_{m=-n}^{n} i^{n+1} \left[a_{mn}^l \bar{N}_{mn}^{(3)l} + b_{mn}^l \bar{M}_{mn}^{(3)l} \right] \tag{1}$$

$$E_{int}^l = -E_0 \sum_{n=1}^{\infty} \sum_{m=-n}^{n} i^{n+1} \left[d_{mn}^l \bar{N}_{mn}^{(1)l,int} + c_{mn}^l \bar{M}_{mn}^{(1)l,int} \right]$$

where:

$$\bar{M}_{mn}^{(l)} = \left[\hat{e}_\theta i \pi_{mn} \left(\theta \right) - \hat{e}_\varphi \tau_{mn} \left(\theta \right) \right] z_n^{(l)} \left(\rho \right) \times \exp \left(im\varphi \right),$$

$$\bar{N}_{mn}^{(l)} = \left\{ \hat{e}_r n \left(n+1 \right) P_n^m \left(\cos \theta \right) \frac{z_n^{(l)} \left(\rho \right)}{\rho} + \left[\hat{e}_\theta \tau_{mn} \left(\theta \right) + \hat{e}_\varphi i \pi_{mn} \left(\theta \right) \right] \frac{\left[\rho z_n^{(l)} \left(\rho \right) \right]'}{\rho} \right\} \times \exp \left(im\varphi \right) \tag{2}$$

Without loss of generality, an incident EM plane wave propagating in positive z direction, with linear polarization defined by β_p angle is considered in this paper to illuminate the multi-sphere system. For mentioned type of incident wave, expansion coefficients have simple form [3]:

$$q_{mn}^l = -\exp\left(ikZ^l\right) m\delta_{|m|,1}\frac{\sqrt{2n+1}}{2}\exp\left(-im\beta_p\right),$$
$$p_{mn}^l = \exp\left(ikZ^l\right) m\delta_{|m|,1}\frac{\sqrt{2n+1}}{2}\exp\left(-im\beta_p\right) \tag{3}$$

At the surface of the lth dielectric sphere because there are not any magnetic or electric charges, internal and external EM fields should cancel each other, so the boundary condition at the surface is demonstrated below:

$$\left(E^i + E^s - E^I\right) \times \hat{r} = \left(H^i + H^s - H^I\right) \times \hat{r} = 0 \tag{4}$$

Surface boundary conditions satisfies Eq. (4) in terms of EM fields' expansions in spherical coordinates as Eq. (1) GMMT coefficients are obtained as a function of classical Mie Theory coefficients:

$$a_{mn}^l = a_n^l p_{mn}^l, \quad b_{mn}^l = b_n^l q_{mn}^l, \quad c_{mn}^l = c_n^l q_{mn}^l, \quad d_{mn}^l = d_n^l p_{mn}^l \tag{5}$$

2.2. Translational Addition Theorem

Notice that incident EM field on the lth sphere is the sum of primary excitation field and the EM field scattered by other spheres. Hence, to obtain scattering coefficients of the lth sphere, the scattered field of rest spheres should be translated to the new coordinate system originated in the center of the lth sphere. This event is possible by the help of *Translational Addition Theorem* [11]. In this method, scattered field of an isolated sphere will be considered as incident field to mentioned origin sphere, so outward VSWF turns to inward one.

$$\bar{M}_{mn}^{(3)}(l) = \sum_{\nu=0}^{\infty}\sum_{\mu=-\nu}^{\nu}\left(A_{\mu\nu}^{mn}(l,j)M_{\mu\nu}^{(1)}(j) + B_{\mu\nu}^{mn}N_{\mu\nu}^{(1)}(j)\right),$$
$$\bar{N}_{mn}^{(3)}(l) = \sum_{\nu=0}^{\infty}\sum_{\mu=-\nu}^{\nu}\left(B_{\mu\nu}^{mn}(l,j)M_{\mu\nu}^{(1)}(j) + A_{\mu\nu}^{mn}N_{\mu\nu}^{(1)}(j)\right) \tag{6}$$

Eq. (6) demonstrates the outward VSWF as the sum of inward VSWF in terms of translational coefficients. $A_{\mu\nu}^{mn}$ and $B_{\mu\nu}^{mn}$ are mentioned translational coefficients [12]:

$$A_{\mu\nu}^{mn} = (-1)^\mu i^{\nu-n}\frac{2\nu+1}{2\nu(2\nu+1)}\sum_{p=|n-\nu|}^{n+\nu}(-i)^p \times [n(n+1) + \nu(\nu+1) - p(p+1)]$$
$$\times a(m,n,-\mu,\nu,p) h_p^{(1)}(kd_{j,l}) \times P_p^{m-\mu}(\cos\theta_{j,l})\exp[i(m-\mu)\phi_{j,l}]$$
$$B_{\mu\nu}^{mn} = (-1)^\mu i^{\nu-n}\frac{2\nu+1}{2\nu(2\nu+1)}\sum_{p=|n-\nu|}^{n+\nu}(-i)^p \times b(m,n,-\mu,\nu,p,p-1) h_p^{(1)}(kd_{j,l}) \tag{7}$$
$$\times P_p^{m-\mu}(\cos\theta_{j,l})\exp[i(m-\mu)\phi_{j,l}]$$

As seen in Eq. (7), it is obvious that translational coefficients are functions of sphere's coordinates; $d_{j,l}$ is the distance between two arbitrary spheres; $\theta_{j,l}$ and $\varphi_{j,l}$ are differential elevation and azimuth angles of two mentioned spheres. To achieve the absolute value of translational coefficients, *Gaunt Coefficients* should be calculated primarily.

2.3. Gaunt Coefficients

Gaunt coefficients are integral expressions of Associated Legendre functions which are employed to translate origins in different coordinate systems. As mentioned in Eq. (7), expressions for $a(m,n,-\mu,\nu,p)$ and $b(m,n,-\mu,\nu,p,p-1)$ are considered as Gaunt coefficients [13]. These two

expressions are correlated functions, so here $a(m, n, \mu, \nu, p)$ results will be illustrated in table which leads to obtaining $b(m, n, \mu, \nu, p, p-1)$ results, subsequently.

$$a\left(m, n, \mu, \nu, p\right) = \frac{2p+1}{2} \frac{(p-m-\mu)!}{(p+m+\mu)!} \times \int_{-1}^{1} P_n^m\left(x\right) P_\nu^\mu\left(x\right) P_p^{m+\mu}\left(x\right) dx \tag{8}$$

Table 1 shows the comparison between 3jm method, REC-G recursive theme and designed method in this paper [13]. Results show extremely good agreement that proves efficiency of the algorithm in this paper.

Table 1. Calculation of gaunt coefficients.

			$a(m, n, \mu, \nu, p)$		
m, n	μ, ν	p	3jm Method	REC-G Method	Paper Results
$m = 7,$ $n = 42$	$\mu = -15,$ $\nu = 44$	$p = 20$	$-0.200951835283E - 04$	$-0.200951835283E - 04$	$-2.009518352830E - 05$
$m = 7,$ $n = 42$	$\mu = -15,$ $\nu = 44$	$p = 12$	$0.256949806872E - 06$	$0.256949806872E - 06$	$2.569498068717E - 07$
$m = 6,$ $n = 50$	$\mu = 8,$ $\nu = 62$	$p = 44$	$0.182562971139E + 00$	$0.182562971137E + 00$	0.182562971139
$m = 6,$ $n = 50$	$\mu = 8,$ $\nu = 62$	$p = 36$	$-0.420617949011E + 01$	$-0.420617949015E + 01$	-4.20617949011
$m = 20,$ $n = 66$	$\mu = 36,$ $\nu = 84$	$p = 74$	$0.113220844079E + 02$	$0.113220844079E + 02$	11.3220844078

2.4. Amplitude Scattering Matrix

Amplitude scattering matrix demonstrates relation between scattered and incident EM field components in both parallel and perpendicular polarizations [3]. For a plane wave propagating in positive z direction in Cartesian coordinates scattering matrix has the form below [12]:

$$\begin{bmatrix} E_{\|sca} \\ E_{\perp sca} \end{bmatrix} = \frac{e^{jk(r-z)}}{jkr} \begin{bmatrix} S_2 & S_3 \\ S_4 & S_1 \end{bmatrix} \begin{bmatrix} E_{\|inc} \\ E_{\perp inc} \end{bmatrix} \tag{9}$$

Scattering intensities for different elevation (θ) and azimuth angles (φ) are defined in terms of the scattering matrix elements:

$$i_{11}\left(\theta, 0^\circ\right) = \left| S_1^{(90^\circ)}\left(\theta, 0^\circ\right) \right|^2, \quad i_{22}\left(\theta, 0^\circ\right) = \left| S_2^{(0^\circ)}\left(\theta, 0^\circ\right) \right|^2 \tag{10}$$

Scattering intensities shown in Eq. (10) are in the cross-polarization with each other. According to GMMT scattering coefficients amplitude matrix elements can be calculated directly. Amplitude scattering matrix provides significant information about scattering properties of the multi-sphere system [12]. Radar Cross Section (RCS) will be obtained directly in terms of opposite scattering intensities [14]:

$$\sigma_{VV} = \frac{\lambda^2}{4\pi^2} i_{11} \quad \sigma_{HH} = \frac{\lambda^2}{4\pi^2} i_{22} \tag{11}$$

Differential Radar Cross Section is the average of differential cross sections in vertical and horizontal polarizations [14]:

$$\sigma_{sca} = \frac{\lambda^2}{8\pi^2}\left(i_{11} + i_{22}\right) \tag{12}$$

2.5. Bulk Model for Particles Much Smaller Than Wavelength

Mie Theory is a method to investigate scattering by spherical particles, with size parameter of $x = 2\pi r/\lambda \approx 1$ where λ is the wavelength of incident EM field. For spheres with the size parameter

of $x \ll 1$ Mie Theory's accuracy decreases, so in this situation Bulk model will be helpful for getting accurate results. Since GMMT is the generalization of classical Mie theory, bulk model is applicable to GMMT, similarly. Bulk model employed in this paper is based on Effective Medium Theory where small particles compared to wavelength are considered as electrical dipoles [15]. Aggregates of these dipoles which are specifically oriented can be modeled as a coarser particle, and in later discussion, it will be illustrated that specific orientation is not necessary, and random orientation can be applied to this approximation. Bulk model analysis illustrates small particles as spheres with the electrical permittivity of ε_r specifically oriented in a lattice which altogether are modeled by a new sphere coarser than them with ε_{eff} confined in a medium introduced by ε_H which is illuminated by a plane wave. The expression for ε_{eff} follows the effective medium theory, where [15]:

$$\varepsilon_{eff} = \varepsilon_H + \frac{3f\varepsilon_H \left[\dfrac{\varepsilon_r - \varepsilon_H}{\varepsilon_r + 2\varepsilon_H} \right]}{1 - f \left[\dfrac{\varepsilon_r - \varepsilon_H}{\varepsilon_r + 2\varepsilon_H} \right]} \tag{13}$$

In Eq. (13), f is the fraction volume occupied by tiny particles. In terms of the discussed bulk model, GMMT application is validated for particles much smaller than incident wavelength.

3. EXERTED FORCES ON SPHERICAL PARTICLES

This section demonstrates the absolute value of exerted force on the particles besides the direction of motion. EM exerted force value is calculated according to Discrete Dipole Approximation [6].

3.1. Discrete Dipole Approximation

As discussed before, particles much smaller than wavelength can be considered as electrical dipoles. Each particle is defined by a position vector r_l and electrical polarization α_l, so the dipole momentum can be directly obtained by dipole polarization [6]:

$$P_l = \alpha_l E_l \tag{14}$$

Here E_l is the electric field on the lth particle and defined by expression below:

$$E_l = E_{inc,l} - \sum_{k \neq l} A_{lk} P_k \quad A_{lk} = \frac{\exp(ikr_{lk})}{r_{lk}} \left[k^2 \left(\hat{r}_{lk}\hat{r}_{lk} - I_3 \right) + \frac{ikr_{lk} - 1}{r_{lk}^2} \left(3\hat{r}_{lk}\hat{r}_{lk} - I_3 \right) \right] \tag{15}$$

Similar to translational addition theorem A_{lk} translates scattered field by rest spheres on the lth one.

3.2. Electromagnetic Force Exerted on a Dipole

To derive the EM force exerted on a dipole, first electrical polarization of dipole should be calculated. *A-1 term* method is a proper solution to achieve electrical polarization in terms of Mie scattering coefficient [16]. In this method, polarization can be obtained directly by first Mie scattering coefficient a_1 which suits GMMT.

$$\alpha_l = i\frac{3a_1}{2k^3} \tag{16}$$

In Eq. (16), k is propagation constant in free space. By substitution of Eq. (16) into Eq. (14), dipole momentum will be calculated. The electromagnetic force exerted on a dipole due to EM field is a function of electrical and magnetic field as below [17]:

$$F = (p \cdot \nabla) E + p \times (\nabla \times E) + \frac{d}{dt} (p \times B) \tag{17}$$

By neglecting the effect of magnetic field according to smaller amplitude than electrical field which is a reasonable approximation, Eq. (17) will have a simple form:

$$F = \sum_i p_i \nabla E_i \quad i = x, y, z \tag{18}$$

As seen in Eq. (18), gradient operates on a vector, then result will be a 3×3 dyadic which illustrates each component of force due to any component of electrical field. In this way, all the possible conditions have been considered for anisotropic scattering medium.

3.3. Electrical Properties of Particles

Particles are considered as dielectric spheres in this paper, so dielectric permittivity, dielectric loss and electrical conductivity are the main electrical properties of the spherical particles. Random quantities are considered for the particles' dielectric permittivity and electrical conductivity. The programmed algorithm is not limited to the particles' material and their orientation. It is a comprehensive algorithm for all types of materials and orientations. As an example, electrical properties of mentioned particles are demonstrated through several tables in later sections.

4. NUMERICAL RESULTS

This section provides numerical results discussed before about particles. Radar cross section, bulk model efficiency and forces exerted on particles are the parameters which will be calculated in the next sections. Two different conditions are considered to simulate with particles' electrical properties at different microwave frequencies. Both simulations have been verified by bulk model to analyze smaller particles than wavelength. Operating system is Core i5 M460, 2.53 GHz CPU with 4GB DDR 3 RAM memory. Software package is MATLAB besides Computer Simulation Technology (CST). Designed algorithm to calculate RCS and exerted force programmed by MATLAB and bulk model analysis are done by CST.

Table 2 demonstrates the configuration of first simulation where particles are millimeter-sized. For a practical viewpoint, electrical properties of particles are considered similar to dust particles [18] for moisture content of 0.079 and can be generalized for any types of particles. The efficiency of programmed algorithm will be discussed in later sections.

Table 2. Configuration of first simulation.

Number of particles	**7**
Electrical permittivity (ε_r)	**4 − j0.7**
Electrical Conductivity (σ)	**-**
Radius	**7 (mm)**
Orientation	**Random**
Frequency	**10 GHz**
Incident wave polarization β_P	**0 (x-polarized)**

Radar cross section for mentioned simulation is calculated through Eq. (12). RCS parameter is illustrated vs. elevation angle (θ) at a fixed azimuth angle $\varphi = 0°$. In terms of RCS results, scattering parameters for aggregate of particles vs. different elevation angles can be extracted. Fig. 1 illustrates the RCS of the 7 arbitrarily oriented spherical particles considered as spheres defined in Table 2 illuminating by a linear polarized plane wave.

This configuration is designed for millimeter-sized particles. According to incident wave frequency, these particles are not considered much smaller than wavelength. Bulk model analysis for smaller particles should be employed.

Effective medium theory is employed to apply Mie theory for much smaller particles than wavelength. Fig. 2 shows an example of effective medium theory in which specifically oriented smaller particles are modeled by a coarser spherical particle with effective permittivity calculated by Eq. (13). Table 3 demonstrates the configuration for bulk model analysis.

Bulk model considered in this section is simulated by CST to compare RCSs of two structures illustrated in Fig. 3. Bulk model reliability is proved by Fig. 3(a) and Fig. 3(b) which compares the
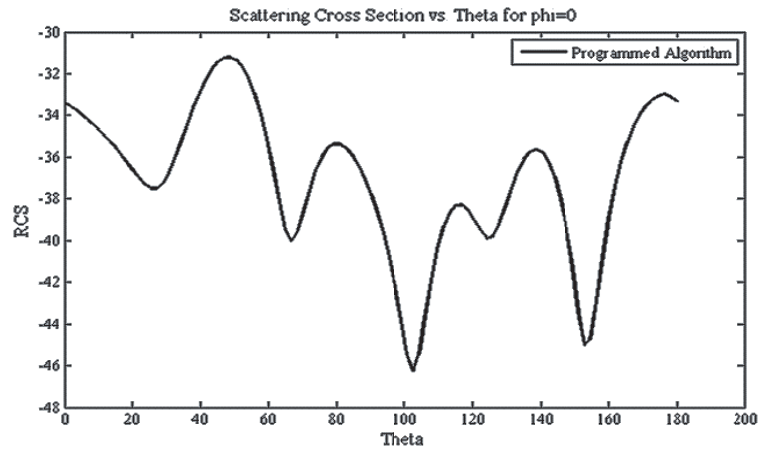
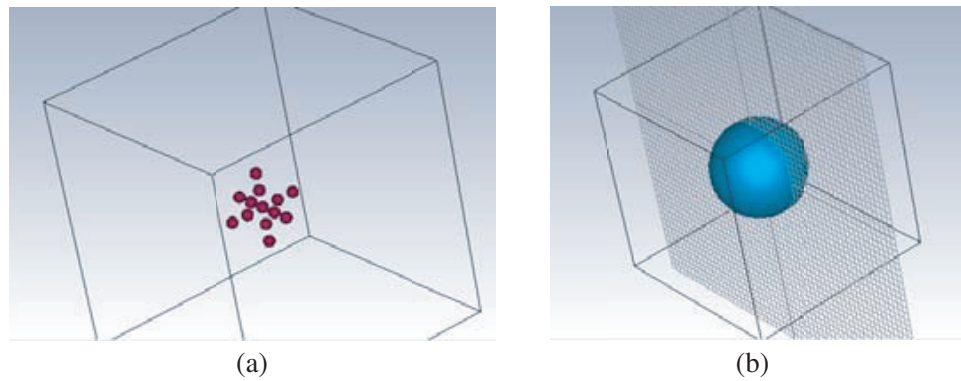**Figure 1.** Radar cross section [dB] vs. elevation angle [Degrees].

(a)   (b)

Figure 2. Bulk model analysis. (a) Original model. (b) Bulk model.

Table 3. Configuration of bulk model analysis.

Number of particles	**13**
Electrical permittivity (ε_r)	**4**
Electrical Conductivity (σ)	**-**
Particle Radius	**1 (mm)**
Distance between particles	**3 (mm)**
Bulk model radius	**7 (mm)**
Effective permittivity (ε_{eff})	**1.1**
Frequency	**10 GHz**
Incident wave polarization β_P	**0 (x-polarized)**

RCSs of two mentioned structures. In later sections, the effect of electrical conductivity will be discussed. RCS comparison is done vs. elevation angle at fixed azimuth angles ($\varphi = 0°, \varphi = 90°$).

After checking the reliability of bulk model analysis, the last part of calculations is dedicated to force exerted on particles. Mie theory and DDA are employed to obtain dipole polarization and forces exerted on particles. As mentioned in Eq. (18), result is a matrix that demonstrates the components of electrical Lorentz force. Configuration discussed in Table 2 is considered once more. Fig. 4(a) illustrates
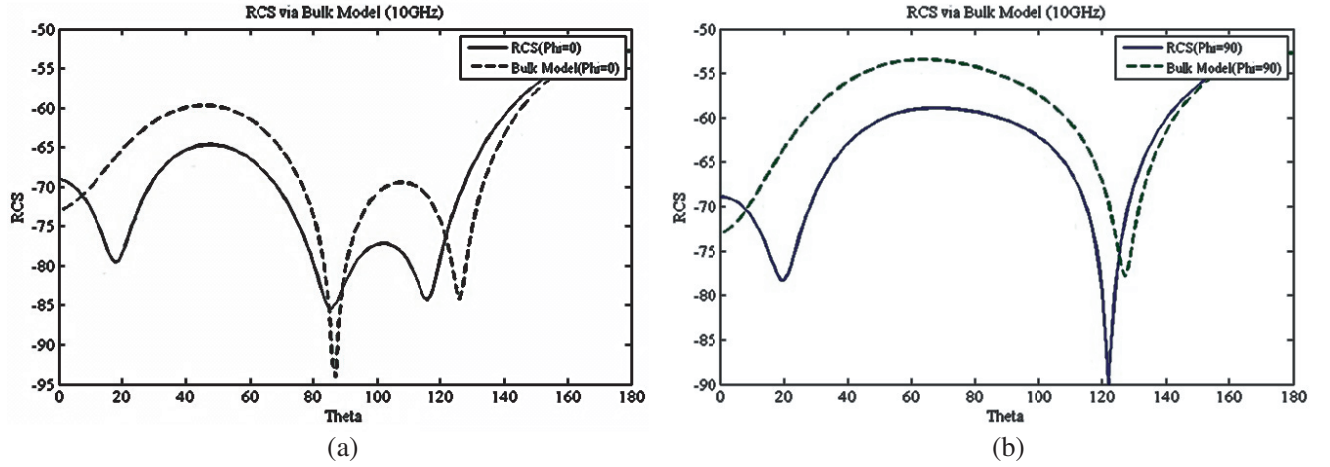
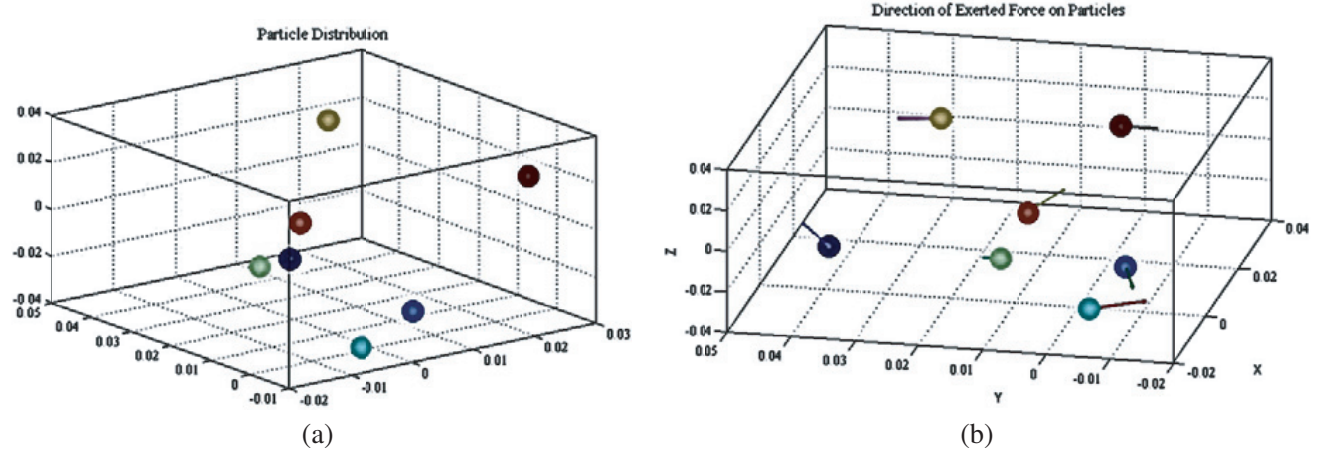**Figure 3.** RCS [dB] comparison of original structure vs. bulk model. (a) $\varphi = 0°$. (b) $\varphi = 90°$.

Figure 4. Orientation of particles. (a) Distribution. (b) Direction of motion.

Table 4. Components of exerted force.

Particle no.	x (mm)	y (mm)	z (mm)	$F_x(N)$	$F_y(N)$	$F_z(N)$
1	13.9	42.9	−35.9	9.12E − 08	1.52E − 07	2.18E − 07
2	2.21	−6.8	−21.2	−3.28E − 06	−1.26E − 06	8.78E − 08
3	−3.56	−2.59	−36	3.04E − 08	−5.23E − 08	1.81E − 09
4	−12.4	9	−3.4	2.86E − 06	2.42E − 06	−3.72E − 06
5	7.6	23.5	38.5	7.84E − 05	2.42E − 04	−1.48E − 04
6	−8	5.8	14.4	2.23E − 03	−1.46E − 03	1.75E − 03
7	25.4	0	19.1	4.53E − 05	−4.17E − 05	−5.7E − 05

the orientation of particles. Accordingly, Fig. 4(b) demonstrates direction of Lorentz force exerted on particles. Positions of particles and component of forces exerted on particles are demonstrated in Table 4.

Considered dipoles in bulk model analysis, which are particles much smaller than wavelength, move in the direction of bulk sphere. Since mentioned dipoles are much smaller than wavelength of incident wave, electrical field on coarse bulk model particle can be approximated the same as electrical
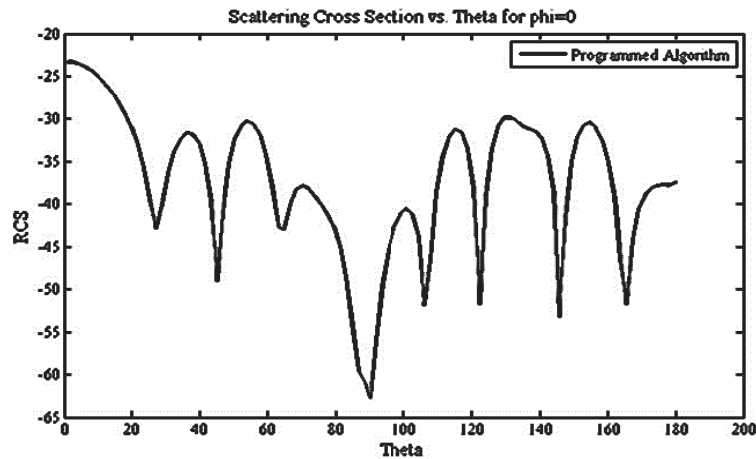
Figure 5. Radar cross section [dB] vs. elevation angle [Degree].

field on dipole position, then the total force exerted on bulk particle also stimulates smaller particles. Millimeter-sized particles' motion due to microwave propagation is discussed in last section. Now a new simulation for micrometer-sized particles will be considered, and it is a practical one for environmental protection.

Figure 5 illustrates RCS of configuration in Table 5 vs. elevation angle (θ) at a fixed azimuth angle $\varphi = 0°$ based on GMMT.

Similarly, bulk model analysis as in Fig. 6 is employed for micrometer-sized particles where configurations of original and modeled particles are shown in Table 6 in detail.

Table 5. Configuration of second simulation.

Number of particles	**10**
Electrical permittivity (ε_r)	**3.8 − j0.9**
Electrical Conductivity (σ)	**0.1 (s/m)**
Radius	**1 (mm)**
Orientation	**Random**
Frequency	**20 GHz**
Incident wave polarization β_P	**0 (x-polarized)**

Table 6. Configuration of bulk model analysis.

Number of particles	**19**
Electrical permittivity (ε_r)	**3.8**
Electrical Conductivity (σ)	**0.1 (s/m)**
Particle Radius	**0.1 (mm)**
Distance between particles	**0.3 (mm)**
Bulk model radius	**1 (mm)**
Effective permittivity (ε_{eff})	**1.1**
Frequency	**20 GHz**
Incident wave polarization β_P	**0 (x-polarized)**

(a)   (b)

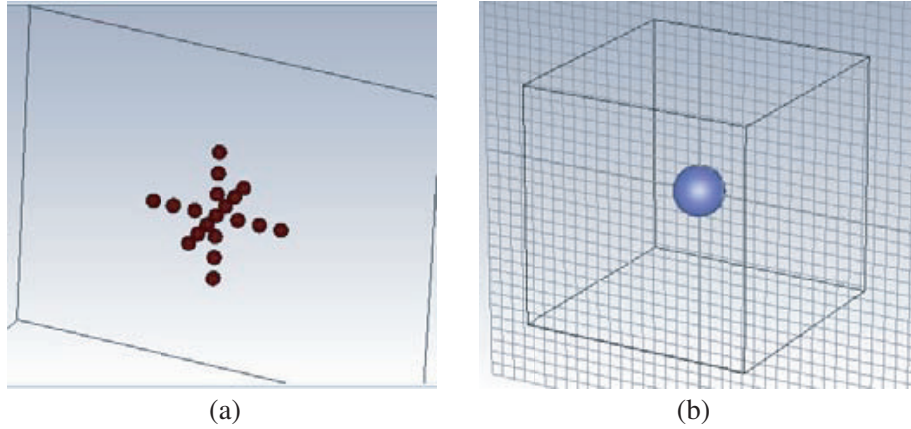**Figure 6.** Bulk model analysis. (a) Original model. (b) Bulk model.

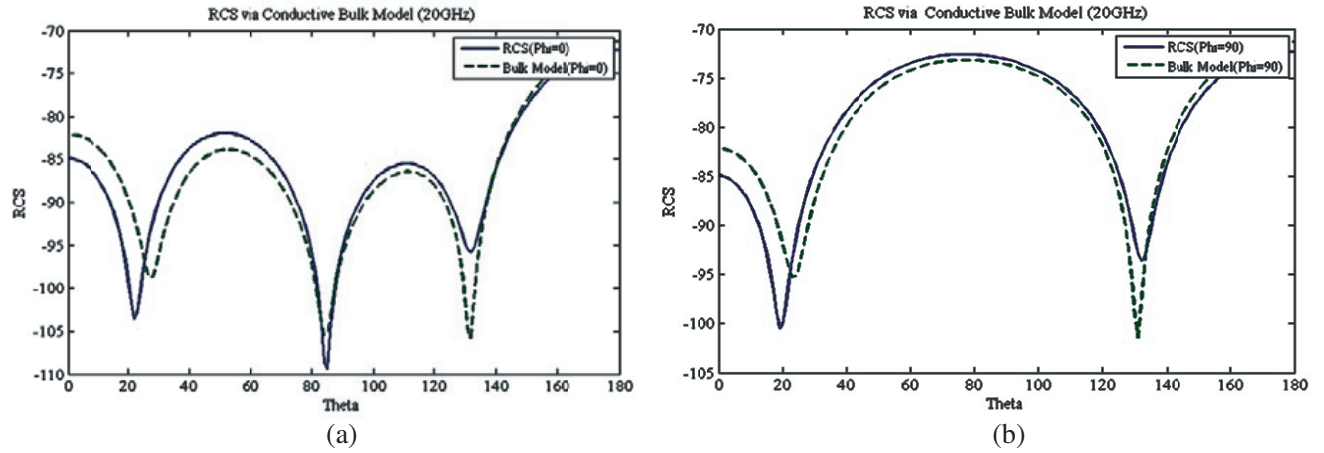(a)   (b)

Figure 7. RCS [dB] comparison of original structure vs. bulk model for (a) $\varphi = 0°$, (b) $\varphi = 90°$.

The next step is to validate effective medium theory involvement in multi-particle scattering by CST simulation of original and modeled structure at 20 GHz frequency. Electrical conductivity is also involved in improving the reliability of bulk model analysis. Results show better agreement than before when conductivity of 0.1 (s/m) is considered. Consuming of conductivity is a realistic definition of natural particles in practice.

Simulation done by CST confirms the prediction of the writers in conductivity involvement which leads to more accurate results. Fig. 7 compares the RCS of original model with the conductive bulk model for two different azimuth angles at 20 GHz, and the results show great agreement by considering electrical conductivity for the desired bulk model. As discussed before, specific and regular orientation in bulk model analysis is not a necessity. Fig. 6 demonstrates a regular orientation, but anisotropic or arbitrary orientation is also simulated in this paper.

Configuration of Fig. 8 is demonstrated in Table 7 in detail. Despite primary simulations in this condition particles in original model are arbitrary oriented, so there is not any regular form in orientation. Distance between particles is random. Results shown in later parts claim that reliability of bulk model analysis is a direct function of fraction volume, not orientation, which means that the more particles are involved in specific medium, the better results occur for bulk model analysis. So, accuracy of approximation is obedient of fraction volume ratio. RCS calculations are illustrated in Fig. 9(a) and Fig. 9(b).

Motion of particles oriented in Fig. 10(a) is illustrated in Fig. 10(b), and the position of particles besides components of exerted force is shown in Table 8.
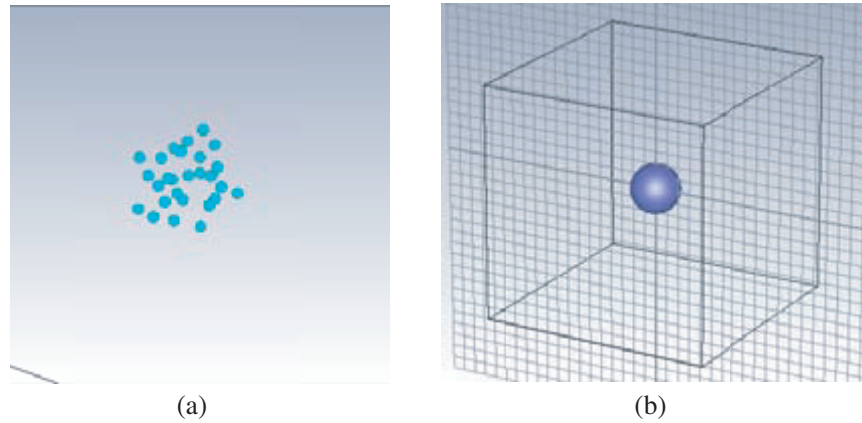
(a)   (b)

Figure 8. Arbitrary bulk model analysis. (a) Original model. (b) Bulk model.
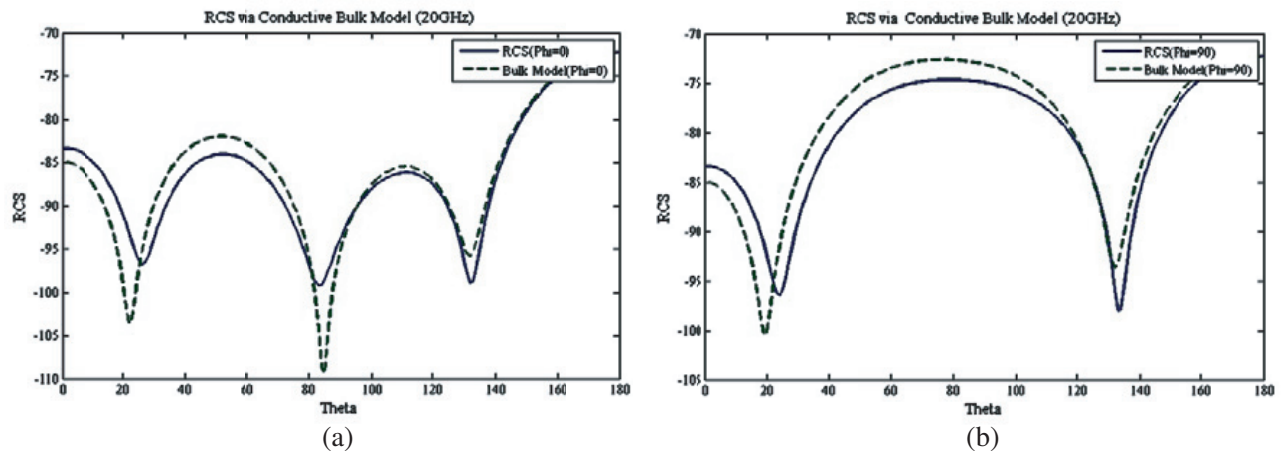

(a)   (b)

Figure 9. RCS [dB] comparison of original arbitrary structure vs. bulk model for (a) $\varphi = 0°$, (b) $\varphi = 90°$.

Table 7. Configuration of bulk model analysis.

Number of particles	**28**
Electrical permittivity (ε_r)	**3.8**
Electrical Conductivity (σ)	**0.1 (s/m)**
Particle Radius	**0.1 (mm)**
Distance between particles	**random**
Bulk model radius	**1 (mm)**
Effective permittivity (ε_{eff})	**1.1**
Frequency	**20 GHz**
Incident wave polarization β_P	**0 (x-polarized)**

Exerted force on each particle also acts on smaller particles which are altogether modeled by a bulk particle. Direction of exerted force on dipoles can be approximated by the direction of force exerted on bulk particle. Electromagnetic field inside the modeled particle and on located smaller particles is a ratio of EM field illuminating the bulk particle. Hence, since direction of exerted force is related to gradient of EM field on particle, direction of force exerted on micrometer-sized particles is parallel to direction of exerted force on bulk particle.
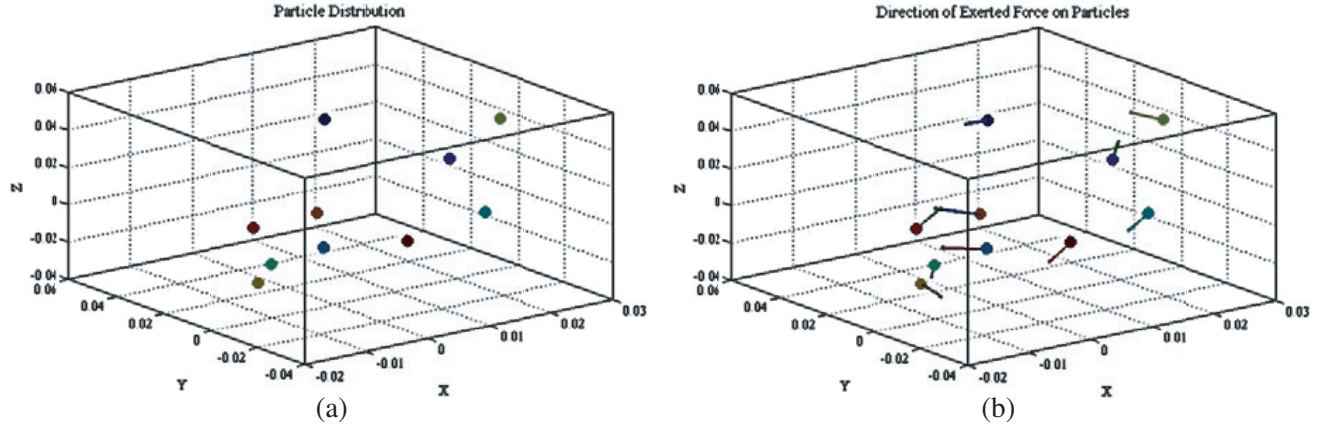
Figure 10. Orientation of particles. (a) Distribution. (b) Motion of direction.

Table 8. Components of exerted force.

Particle no.	x (mm)	y (mm)	z (mm)	$F_x(N)$	$F_y(N)$	$F_z(N)$
1	8.5	26.2	41.1	$-3.6E-07$	$-3.35E-07$	$2.83E-07$
2	8.6	-26.6	44.4	$4.86E-08$	$9.48E-08$	$4.76E-08$
3	-2.4	-1.7	-7.2	$-1.64E-06$	$3.09E-06$	$-6.29E-08$
4	24.5	0	-8	$-8.11E-08$	$6.51E-08$	$-2.74E-07$
5	-14	-10.2	-4	$1.6E-08$	$8.48E-08$	$-2.82E-07$
6	27	0	40.3	$-5.92E-08$	$2.45E-07$	$4.38E-08$
7	-9.4	6.8	-24.9	$-3.63E-09$	$-5.68E-07$	$-2E-07$
8	15.3	47.1	-23.5	$-1E-08$	$1.51E-08$	$7.76E-09$
9	-10	7.3	4.78	$4.66E-07$	$2.46E-08$	$9.13E-07$
10	5.53	-17	-2.1	$-4.86E-07$	$-6.93E-09$	$-1.17E-06$

5. INCIDENT WAVE EFFECT ON EXERTED FORCE

5.1. Wave Amplitude and Polarization

Simulation in primary sections, all are done by a normalized incident wave illumination multi-particle system. Suppose that amplitude of incident wave is not normalized, then by Eq. (1) it can be understood that E_0 is a fixed parameter, and it is not a matter of orientation or particle properties. In terms of Eq. (18) it is obvious that amplitude of incident wave has direct effect on absolute value of exerted force but not direction of motion.

Back to configuration of Table 5 for orientation and properties of particles, polarization of incident wave can be discussed by change of polarization angle β_P. As an example, $\beta_P = 45°$ is simulated in this paper. Orientation and configuration is the same as previous simulation, and new simulation is devoted just to investigate polarization effect. Table 9 demonstrates components of exerted force as polarization changes.

5.2. Wave Types

Incident wave can be considered in various types as plane wave, cylindrical wave or spherical wave. For a plane wave expansion coefficients are obtained by Eq. (3). Otherwise, coefficients follow the expressions

Table 9. Components of exerted force.

Particle no.	$x(mm)$	$y(mm)$	$z(mm)$	F_x	F_y	F_z
1	8.5	26.2	41.1	$-1.84\text{E} - 07$	$3.27\text{E} - 07$	$-1.62\text{E} - 07$
2	8.6	−26.6	44.4	$-4.51\text{E} - 07$	$3.03\text{E} - 07$	$3.11\text{E} - 07$
3	−2.4	−1.7	−7.2	$-1.79\text{E} - 05$	$-1.07\text{E} - 05$	$8.99\text{E} - 06$
4	24.5	0	−8	$-1.04\text{E} - 08$	$5.94\text{E} - 07$	$6.89\text{E} - 08$
5	−14	−10.2	−4	$-3.1\text{E} - 07$	$7.52\text{E} - 07$	$-8.84\text{E} - 07$
6	27	0	40.3	$-1.3\text{E} - 06$	$5.88\text{E} - 07$	$-9.13\text{E} - 07$
7	−9.4	6.8	−24.9	$-2.38\text{E} - 06$	$-9.43\text{E} - 08$	$9.02\text{E} - 07$
8	15.3	47.1	−23.5	$-2.11\text{E} - 07$	$-1.32\text{E} - 08$	$-1.92\text{E} - 08$
9	−10	7.3	4.78	$-1.12\text{E} - 06$	$8.59\text{E} - 07$	$-3.41\text{E} - 06$
10	5.53	−17	−2.1	$-3.98\text{E} - 08$	$-1.25\text{E} - 07$	$6.52\text{E} - 07$

below:

$$
\begin{aligned}
p_{mn} &= \frac{i\int_0^{2\pi}\int_0^{\pi}\bar{E}_{inc}\cdot N_{mn}^{(1)*}\left(\rho,\theta,\varphi\right)\sin\theta d\theta d\varphi}{E_0 i^n\dfrac{(n-m)!}{(n+m)!}\left(2n+1\right)\int_0^{2\pi}\int_0^{\pi}\left|N_{mn}^{(1)}\left(\rho,\theta,\varphi\right)\right|^2\sin\theta d\theta d\varphi} \\[2mm]
q_{mn} &= \frac{i\int_0^{2\pi}\int_0^{\pi}\bar{E}_{inc}\cdot M_{mn}^{(1)*}\left(\rho,\theta,\varphi\right)\sin\theta d\theta d\varphi}{E_0 i^n\dfrac{(n-m)!}{(n+m)!}\left(2n+1\right)\int_0^{2\pi}\int_0^{\pi}\left|M_{mn}^{(1)}\left(\rho,\theta,\varphi\right)\right|^2\sin\theta d\theta d\varphi}
\end{aligned}
\tag{19}
$$

For any type of incident wave expansion coefficients will be obtained properly. Procedure for linear plane wave should be followed to calculate exerted force on particles by other types of incident wave.

6. EFFICIENCY OF PROGRAMMED ALGORITHM

The designed algorithm is proposed to calculate RCS and exerted force, merely. The process time of designed two simulations is demonstrated in Table 10 accurately. The more complex the structure is, the more time the process is needed.

Table 10. Process time of programmed algorithm.

No.	Number of particles	Orientation	Process Time
1	7	Random	506 sec.
2	10	Random	990 sec.

7. CONCLUSION

Electromagnetic wave abilities in movement of small particles are discussed in this paper. The absolute value and direction of exerted Lorentz force on particles are demonstrated in detail. Components of exerted force are illustrated in various tables. Microwave propagation in random medium and motion of small spherical particles are calculated by a programmed MATLAB algorithm according to microwave radiation in two arbitrary frequencies. Electromagnetic scattering parameters for aggregates of millimeter and micrometer-sized spheres besides random electrical properties of particles are important parts of this paper. Practical application of EM deviation for environmental protection is investigated

through soil electrical properties applied to spherical particles. Mie theory and DDA are employed to analyze multi-particle scattering problem for particles with sizes comparable to wavelength of incident wave. For particle much smaller than incident wavelength, a bulk model based on effective medium theory is designed and validated by several simulations done by CST. The last section is devoted to discussing effects of wave amplitude, polarization and wave types on deviation of particles.

REFERENCES

1. Tsang, L., J. A. Kong, and K.-H. Ding, *Scattering of Electromagnetic Waves, Theories and Applications*, Vol. 27, John Wiley & Sons, 2004.

2. Ishimaru, A., *Electromagnetic Wave Propagation, Radiation, and Scattering*, Prentice-Hall, 1991.

3. Xu, Y.-L., "Electromagnetic scattering by an aggregate of spheres," *Applied Optics*, Vol. 34, 4573–4588, 1995.

4. Xu, Y.-L., "Scattering Mueller matrix of an ensemble of variously shaped small particles," *JOSA A*, Vol. 20, 2093–2105, 2003.

5. Mishchenko, M. I., L. D. Travis, and D. W. Mackowski, "*T*-matrix computations of light scattering by nonspherical particles: A review," *Journal of Quantitative Spectroscopy and Radiative Transfer*, Vol. 55, 535–575, 1996.

6. Draine, B. T. and P. J. Flatau, "Discrete-dipole approximation for scattering calculations," *JOSA A*, Vol. 11, 1491–1499, 1994.

7. Dong, Q.-F., Y.-L. Li, J.-D. Xu, H. Zhang, and M.-J. Wang, "Effect of sand and dust storms on microwave propagation," *IEEE Transactions on Antennas and Propagation*, Vol. 61, 910–916, 2013.

8. Kimura, H., H. Okamoto, and T. Mukai, "Radiation pressure and the Poynting-Robertson effect for fluffy dust particles," *Icarus*, Vol. 157, 349–361, 2002.

9. Kawata, S. and T. Sugiura, "Movement of micrometer-sized particles in the evanescent field of a laser beam," *Optics Letters*, Vol. 17, 772–774, 1992.

10. Xu, Y.-L. and B. Å. Gustafson, "A generalized multiparticle Mie-solution: Further experimental verification," *Journal of Quantitative Spectroscopy and Radiative Transfer*, Vol. 70, 395–419, 2001.

11. Dufva, T. J., J. Sarvas, and J. C.-E. Sten, "Unified derivation of the translational addition theorems for the spherical scalar and vector wave functions," *Progress In Electromagnetics Research B*, Vol. 4, 79–99, 2008.

12. Xu, Y.-L., "Electromagnetic scattering by an aggregate of spheres: Far field," *Applied Optics*, Vol. 36, 9496–9508, 1997.

13. Xu, Y.-L., "Efficient evaluation of vector translation coefficients in multiparticle light-scattering theories," *Journal of Computational Physics*, Vol. 139, 137–165, 1998.

14. Hahn, D. W., "Light scattering theory," Department of Mechanical and Aerospace Engineering, Florida, 2006.

15. Naseem, A., "Computation and analysis of effective permittivity of thin film nanostructures: An effective medium perspective," University of Toledo, 2010.

16. Okamoto, H., "Light scattering by clusters: The al-term method," *Optical Review*, Vol. 2, 407–412, 1995.

17. Novotny, L. and B. Hecht, *Principles of Nano-optics*, Cambridge University Press, 2012.

18. Hallikainen, M. T., F. T. Ulaby, M. C. Dobson, M. A. El-Rayes, and L.-K. Wu, "Microwave dielectric behavior of wet soil — Part 1: Empirical models and experimental observations," *IEEE Transactions on Geoscience and Remote Sensing*, 25–34, 1985.